

Strain-activated edge reconstruction of graphene nanoribbons

Y. C. Cheng,¹ H. T. Wang,² Z. Y. Zhu,¹ Y. H. Zhu,³ Y. Han,³ X. X. Zhang,⁴ and U. Schwingenschlögl^{1,*}

¹*Physical Sciences and Engineering Division, King Abdullah University of Science and Technology, Thuwal 23955-6900, Kingdom of Saudi Arabia*

²*Institute of Applied Mechanics, Zhejiang University, Hangzhou 310027, China*

³*Chemical and Life Sciences and Engineering Division, King Abdullah University of Science and Technology, Thuwal 23955-6900, Kingdom of Saudi Arabia*

⁴*Advanced Nanofabrication, Imaging and Characterization Core Lab, King Abdullah University of Science and Technology, Thuwal 23955-6900, Kingdom of Saudi Arabia*

(Received 15 January 2012; published 17 February 2012)

The edge structure and width of graphene nanoribbons (GNRs) are crucial factors for the electronic properties. A combination of experiment and first-principles calculations allows us to determine the mechanism of the hexagon-hexagon to pentagon-heptagon transformation. GNRs thinner than 2 nm have been fabricated by bombardment of graphene with high-energetic Au clusters. The edges of the GNRs are modified *in situ* by electron irradiation. Tensile strain along the edge decreases the transformation energy barrier. Antiferromagnetism and a direct band gap are found for a zigzag GNR, while a fully reconstructed GNR shows an indirect band gap. A GNR reconstructed on only one edge exhibits ferromagnetism. We propose that strain is an effective method to tune the edge and, therefore, the electronic structure of thin GNRs for graphene-based electronics.

DOI: [10.1103/PhysRevB.85.073406](https://doi.org/10.1103/PhysRevB.85.073406)

PACS number(s): 73.22.Pr, 61.48.Gh, 68.37.Og, 77.80.bn

Graphene has attracted a lot of interest since it first became accessible experimentally in 2004.¹ A substantial portion of the studies is devoted to the physics of graphene nanoribbons (GNRs), due to potential electronics applications. The edge structure and ribbon width are the two major intrinsic factors determining the electronic and magnetic properties.^{2–6} The typical width of GNRs is in the range of 4 to 20 nm.^{5,7,8} Recently, Jin *et al.*⁹ have obtained GNRs by fabricating nearby holes in monolayer graphene by prolonged electron irradiation [see Fig. 1(a)]. This method makes it possible to tailor the width of the GNRs from 2 nm down to even single C chains and to observe the edge structure *in situ*. For decreasing the width of the GNR, it is expected that the edge plays a more and more important role for the structural and electronic properties.

To modify the electronic structure of GNRs several methods have been proposed, such as doping the edge and application of external electric fields.^{10–13} Recently, strain has been suggested as another effective approach to tailor the electronic structure, as it is required for nanoelectromechanical systems.^{14–16} Moreover, it has been predicted theoretically that bending of a ribbon in-plane into a circular arc simulates a magnetic field of 10 T.¹⁷ Tensile (compressive) strain in graphene results in lattice modifications and corresponding phonon mode softening (hardening).¹⁸ However, until now there has been a lack of knowledge about the influence of strain on the edge structure and electronic states of GNRs.

In this Brief Report, we report on the fabrication of ultrathin zigzag GNRs with widths of about 2 nm by bombardment with high-energetic Au clusters. The width of the GNR can be tuned by electron irradiation. We observe by *in situ* transmission electron microscopy (TEM) that the edges can be transformed from a hexagon-hexagon to a pentagon-heptagon pair, where we call GNRs with one and two reconstructed edges semireconstructed (SR) and fully reconstructed (FR), respectively. Density-functional theory reveals that tensile/compressive strain along the edge decreases/increases the transformation energy barrier. The influence of the width of the GNR

on its electronic and magnetic properties is discussed in detail.

Known methods for obtaining GNRs include lithographic patterning of graphene sheets,⁵ chemical sonication,⁷ unzipping of multiwall carbon nanotubes by plasma etching,⁸ as well as bottom-up fabrication.¹⁹ However, the created GNRs unavoidably are polluted by foreign molecules. In addition, the width cannot be controlled and there are problems in characterizing the edge structure. Following the method proposed by Jin *et al.*⁹ to fabricate ultrathin zigzag GNRs, we first have grown a graphene monolayer on a copper foil and then have transferred it to a TEM grid, which avoids substrate effects with the following results. Clean samples can be obtained by annealing in forming gas at 600°C. GNRs are created by bombardment with high-energetic Au clusters generated in a pulse-laser (400 mJ/pulse and 40 ns/pulse) deposition chamber at 10⁻⁸ Torr. The bombarded graphene layer shows holes of various sizes and is found to be free of contaminations [see Fig. 1(c)]. The width of the GNRs produced by this method is typically 2 nm, due to the high density and small radius of the holes. We have monitored *in situ* the behavior of the GNRs under a continuous exposure to electron irradiation by aberration corrected high-resolution TEM with an electron energy of 60 kV.

Our calculations employ the generalized-gradient approximation of the exchange-correlation functional in the Perdew-Burke-Ernzerhof parametrization with ultrasoft pseudopotentials,²⁰ using the Quantum-ESPRESSO package.²¹ We apply periodic boundary conditions and a slab geometry with a vacuum layer of >10 Å thickness. A high cutoff energy of 500 eV and a mesh of 1 × 8 × 1 *k* points are used to achieve a high accuracy. Structural optimization is carried out for all systems until the residual forces have converged to 0.003 eV/Å. The energy barriers are calculated by the climbing-image nudged elastic band (NEB) method,²² which enables us to find the minimum-energy path between given initial and final states of a transition. We describe the

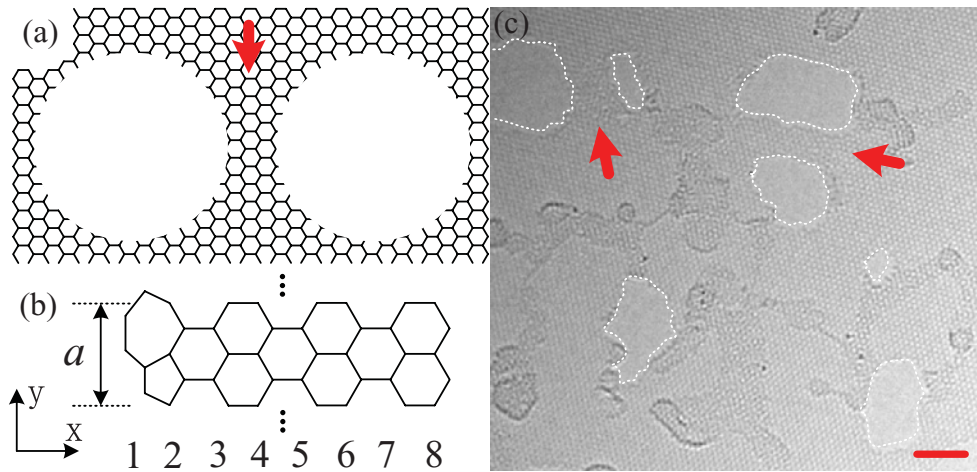


FIG. 1. (Color online) (a) Schematic illustration of a GNR formed by two nearby holes. (b) GNR of width $w = 8$ in the x direction. Calculations have been performed for $w = 2, \dots, 15$. By periodic boundary conditions the length of the GNR is infinite, where a is the lattice parameter along the edge in the y direction. (c) GNRs generated by bombardment with Au clusters using a pulsed high-power laser. The scale bar is 2 nm. In (a) and (c) the red arrows indicate the GNRs.

uniaxial strain by $\varepsilon = (a - a_0)/a_0$, where a and a_0 are the lattice parameters in the strained and nonstrained structures, respectively [see Fig. 1(b)]. We obtain $a_0 = 4.92 \text{ \AA}$, consistent with our experimental value of 4.82 \AA .

Previous 100–200 kV TEM studies of few-layer graphene have indicated that it is difficult to resolve the structure atomically and that a high electron energy can lead to amorphous graphene.^{9,23,24} In order to minimize the electron sputtering effect on the C atoms, we have operated the microscope at 60 kV with a typical electron-beam current density of 100 A/cm^2 . We are able to still achieve a resolution better than 1.1 \AA by introducing a spherical aberration correction

and reducing the energy spread of the electron beam to less than 0.15 eV . In this condition the maximal knock-on energy is 11.3 eV , which is below the threshold for knock-on damage (17 eV) for C atoms in pristine graphene but larger than the threshold for C atoms on the edge ($5.5\text{--}10.5 \text{ eV}$).^{25,26} Our procedure makes it possible to analyze the evolution of the edge structure of the GNRs. Note that electron irradiation can slowly decrease the width of GNRs^{9,27,28} and can induce edge reconstruction.²⁹

Figure 2 shows the edge evolution of a typical GNR through various configurations. We find that the GNR keeps its zigzag direction for more than 10 min when it is thinned by

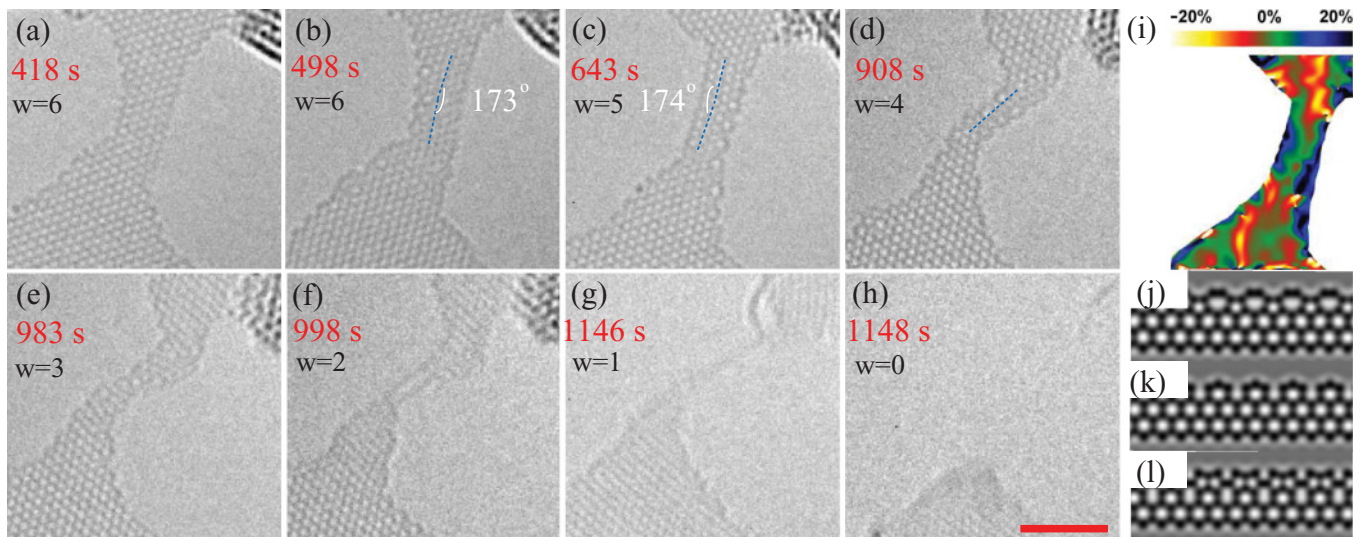


FIG. 2. (Color online) Aberration corrected high-resolution TEM image of a reconstructed zigzag GNR of about 1.5-nm width. The C atoms are resolved as gray spots. The scale bar is 2 nm. (a) Zigzag GNR between two holes ($w = 6$). (b) Left side of the GNR ($w = 6$) reconstructed to a pentagon-heptagon pair series. (c) Right side of the GNR ($w = 5$) reconstructed. (d and e) Both sides reconstructed and the width reduced to $w = 4$ and 3 , respectively. (f and g) GNR transferred to a double and single C chain, respectively. (h) Single C chain finally breaking. (i) Exemplary strain map resulting from the geometric phase analysis of image (c). (j–l) TEM simulations of zigzag edges with pentagon-heptagon pairs, point defects, and stone-wales defects (acceleration voltage 60 kV, spherical aberration $1 \mu\text{m}$, chromatic aberration 1.5 mm , defocus -3 nm , convergence angle 0.15 mrad ³⁰).

electron irradiation. In addition, Fig. 1(c) shows for the edges of both GNRs a zigzag direction. Therefore, our experiment confirms that the zigzag edge is more stable than the armchair edge under electron-beam exposure,²⁷ though the opposite has been predicted theoretically by *ab initio* calculations.^{31,32} The latter two papers also report that reconstruction from a hexagon-hexagon to a pentagon-heptagon configuration can happen spontaneously at room temperature. Sen *et al.*³³ have shown that the reconstruction can be activated via external force. Our TEM simulations in Figs. 2(j)–2(l) point to an edge reconstruction in pentagon-heptagon pairs. Also, molecular-dynamics calculations show that the zigzag and armchair edges are undulated in the out-of-plane direction, whereas the pentagon-heptagon edge is completely flat.³⁴ This implies that the reconstruction results in edge stress. A GNR with lattice parameter a_0 is subject to a compressive (tensile) strain of -1.4 ($+4.4$) nN in the zigzag (FR) edge configuration (for $w > 2$) [see Fig. 3(a)]. Therefore, the assumption^{31,32} that the reconstruction from the zigzag to FR GNR occurs spontaneously at room temperature would imply that the SR GNR bends to the reconstructed side and the FR GNR shrinks. However, our experiments contradict such a scenario. Figure 2(b) shows a $w = 6$ GNR with a reconstructed left side, while Fig. 2(c) shows a $w = 5$ GNR with a reconstructed right side (145 s later). As an example, a strain map in Fig. 2(i) demonstrates strong tensile strain along the GNR edge. We find that the SR GNR bends to the nonreconstructed side [compare the angles in Figs. 2(b) and 2(c)] and that the FR GNR expands by more than 5% [see Figs. 2(d) and 2(e)].

To explain this contradiction, we first examine our experimental setting. One may argue that the reconstruction along the edges of the GNR is activated by the strain introduced by the bombardment of the graphene sheet. From Figs. 2(b)–2(e) we conclude that tensile strain along the edge lowers the transition barrier of the reconstruction. This picture is supported by our calculations. We study a $1 \times 4 \times 1$ supercell and address the transformation of the first hexagon-hexagon pair into a

pentagon-heptagon pair on one side of the GNR ($w = 4$) for different edge strains by the NEB method. The result is shown in Figs. 3(c) and 3(d). Previous findings indicate that this transition barrier is less than 0.7 eV,^{31,32,34} which implies that the reconstruction takes place spontaneously at room temperature. The first step of the reconstruction has the largest barrier (0.8 eV) as compared to further reconstruction steps.³⁴ We find a first transition barrier of $E_0 = 1.12$ eV. Employing transition state theory, we use the relation $k = \nu_G \exp(-E_a/RT)$ with frequency $\nu_G = 5 \times 10^{12} \text{ s}^{-1}$ ³¹ to obtain a rapid transition rate of $7 \times 10^{-6} \text{ s}^{-1}$, which suggests that the reconstruction is impossible at room temperature. However, as the first transition barrier decreases with increasing tensile strain according to Fig. 3(d), a zigzag GNR is transformed into a FR GNR more easily under tensile strain along the edge. Tensile strain increases the initial- and final-state energies but leaves the transition state almost unchanged [see Fig. 3(c)]. Therefore, the transition barrier decreases. Fitting the dependence of the first transition barrier E_b on the strain ε leads to $E_b = a \cdot \varepsilon + E_0$ with $a = -0.21 \text{ eV}/\%$ and $E_0 = 1.12 \text{ eV}$. We estimate that a transition is observed in the TEM images for $\varepsilon > 2\%$.

Figures 2(f) and 2(g) shows double and single C chains, respectively. Figure 2(h) demonstrates the situation after breakage of the single C chain. It is reported that a GNR that is only two to three atoms thin is dominated by the edge atoms, which leads to large structural reconstructions.⁹ However, the details of the latter have not been clarified yet. Experiments indicate that a GNR of width $w > 2$ is still stable [see Figs. 2(a)–2(e)]. By calculating the phonon-dispersion relation in density-functional perturbation theory,³⁵ no negative frequency is obtained for $w > 2$ zigzag, FR, and SR GNRs, which points to stability of such thin GNRs. Figure 5 shows the phonon-dispersion relations of $w = 4$ GNRs. For the zigzag GNR all the branches are below 1580 cm^{-1} , resembling pristine graphene.¹⁸ Extra modes with frequencies around 2000 cm^{-1} are found for the FR and SR GNRs, which mainly correspond to in-plane vibrations along the edge of the two outmost C atoms of the heptagon [see Figs. 4(d) and 4(e)]. These modes can be used to identify the zigzag-to-FR reconstruction by Raman spectroscopy. The zigzag GNR relaxes to a double chain with an energy about 0.8 eV below that of the $w = 2$ FR GNR [compare the insets

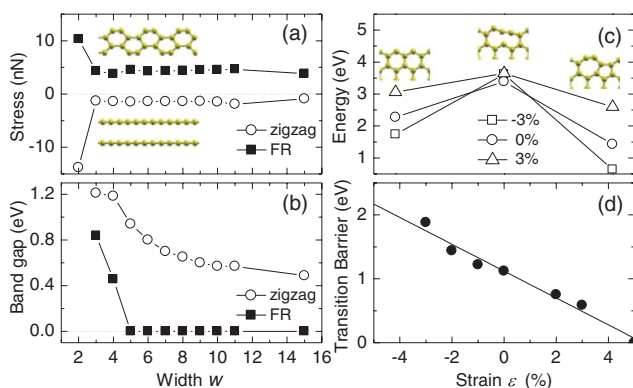


FIG. 3. (Color online) (a) Stress along the GNR edge and (b) band gap for fixed lattice parameter a_0 and width $w = 2, \dots, 15$. The insets in (a) show that the zigzag GNR ($w = 2$) turns into a double chain and the FR GNR ($w = 2$) resembles an armchair GNR. (c) Energy diagram of the initial state, transition state, and final state. (d) Transition barrier for the transformation of the first hexagon-hexagon pair into a pentagon-heptagon pair ($w = 4$) for strain between -5 and 5% . The insets show the structures of the three states.

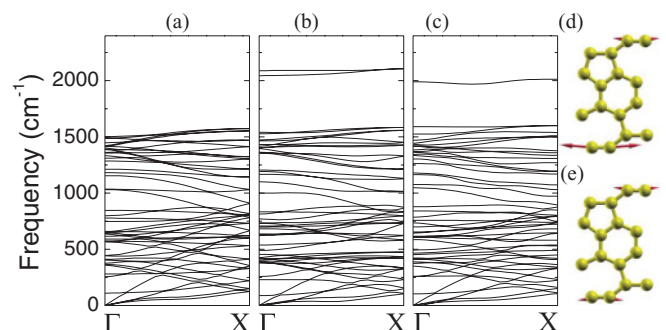


FIG. 4. (Color online) Phonon-dispersion relations of the (a) zigzag, (b) FR, and (c) SR GNRs for $w = 4$. (d) and (e) Atomic displacements of the two FR GNR modes with frequency around 2000 cm^{-1} .

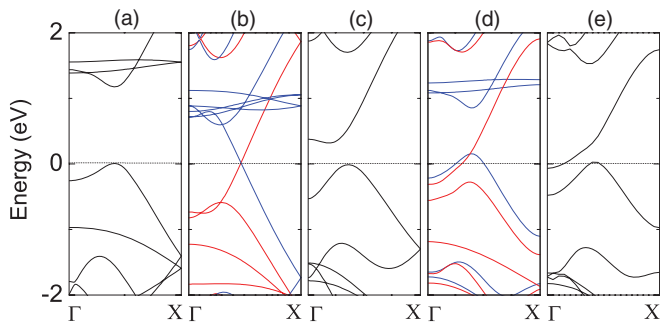


FIG. 5. (Color online) Band structures: (a) AFM $w = 4$ zigzag GNR, (b) FM $w = 4$ zigzag GNR, (c) nonmagnetic $w = 4$ FR GNR, (d) FM $w = 4$ SR GNR, and (e) nonmagnetic $w = 5$ FR GNR. The energy zero is set to be the Fermi energy.

of Fig. 3(a)]. Thus, a $w = 3$ GNR which is turned into a $w = 2$ GNR by electron-beam irradiation ends up as a double C chain. Moreover, Figs. 2(g) and 2(h) demonstrate that the GNR was tensile strained, since the two ends of the remaining single C chain fall apart after the breakage. The effects of tensile strain on single C chains have been analyzed quantitatively by Nair *et al.*³⁶ We note that the edge reconstruction also influences the mechanical strength of GNRs. For $w = 4$ zigzag, FR, and SR GNRs we obtain strengths of 35, 26, and 24 nN, respectively.

The strain-assisted zigzag-to-FR reconstruction in thin GNRs as described above gives rise to a variety of interesting electronic and magnetic properties. When a zigzag GNR becomes thin enough ($w = 4$), the magnetic moments of the two edges develop an antiferromagnetic (AFM) order rather than a ferromagnetic (FM) order, with an appreciable energy difference of 85 meV/cell and magnetic moment of about $3 \mu_B$ /cell. The magnetic ordering opens up an energy gap (1.18 eV for $w = 4$) at the Fermi level [see Fig. 5(a)], and a direct band-gap semiconductor is formed.³ Because the FR

GNR shows an indirect band gap (0.45 eV for $w = 4$) [see Fig. 5(c)], the zigzag-to-FR reconstruction comes along with a direct-to-indirect band-gap transition. In addition, the FR GNR is nonmagnetic due to the absence of dangling bonds. The zigzag-to-SR reconstruction combines a magnetic transition (AFM to FM) with an electronic transition (insulating to metallic) [see Fig. 5(d)]. The zigzag edge of the SR GNR is spin polarized, while the states at the Fermi level mostly belong to the other edge.

In addition, the electronic and magnetic properties depend on the width w of the GNR. When w increases, the exchange interaction between the magnetic moments located at the two edges of a zigzag GNR becomes weaker. Consequently, the band gap decreases rapidly [see Fig. 2(b)]. The FR GNR transforms into a metallic state for $w > 4$ due to an energetic lowering of the states originating from the π bands [see Figs. 4(c) and 4(e)]. The energy difference between the AFM and FM solutions for the zigzag GNR is reduced when w increases. For example, it amounts to 1.1 meV/cell for $w = 15$. This implies that the AFM order of the magnetic moments at the edges of a thick zigzag GNR cannot persist at room temperature.

In conclusion, we have demonstrated the fabrication of ultrathin GNRs (thinner than 2 nm) by bombardment of a graphene sheet with high-energy Au clusters and the *in situ* modification of the edges of the GNRs by electron-beam irradiation. We find that the experimental difficulty to observe a transition of a zigzag GNR edge is due to a large transition barrier of 1.12 eV. Our theoretical results show that tensile strain can be used to activate the transition. We find that ultrathin GNRs are characterized by a complex electronic and magnetic behavior, which is attributed to the strain dependence of the edge reconstruction and the influence of the ribbon width. We propose that strain is an efficient tool for tuning the edge structure and, therefore, the electronic properties of GNRs, to account for the needs of graphene electronics.

*udo.schwingschlögl@kaust.edu.sa

¹K. S. Novoselov, A. K. Geim, S. V. Morozov, D. Jiang, Y. Zhang, S. V. Dubonos, I. V. Grigorieva, and A. A. Firsov, *Science* **306**, 666 (2004).

²K. Nakada, M. Fujita, G. Dresselhaus, and M. S. Dresselhaus, *Phys. Rev. B* **54**, 17954 (1996).

³Y.-W. Son, M. L. Cohen, and S. G. Louie, *Phys. Rev. Lett.* **97**, 216803 (2006).

⁴Y.-W. Son, M. L. Cohen, and S. G. Louie, *Nature (London)* **444**, 347 (2006).

⁵M. Y. Han, B. Özyilmaz, Y. Zhang, and P. Kim, *Phys. Rev. Lett.* **98**, 206805 (2007).

⁶X. Wang, Y. Ouyang, X. Li, H. Wang, J. Guo, and H. Dai, *Phys. Rev. Lett.* **100**, 206803 (2008).

⁷X. Li, X. Wang, L. Zhang, S. Lee, and H. Dai, *Science* **319**, 1229 (2008).

⁸L. Jiao, L. Zhang, X. Wang, G. Diankov, and H. Dai, *Nature (London)* **458**, 877 (2009).

⁹C. Jin, H. Lan, L. Peng, K. Suenaga, and S. Iijima, *Phys. Rev. Lett.* **102**, 205501 (2009).

¹⁰V. Barone, O. Hod, and G. E. Scuseria, *Nano Lett.* **6**, 2748 (2006).

¹¹M. Poetschke, C. G. Rocha, L. E. F. Foa Torres, S. Roche, and G. Cuniberti, *Phys. Rev. B* **81**, 193404 (2010).

¹²E.-J. Kan, Z. Li, J. Yang, and J. G. Hou, *J. Am. Chem. Soc.* **130**, 4224 (2008).

¹³H. Vedala, D. C. Sorescu, G. P. Kotchey, and A. Star, *Nano Lett.* **11**, 2342 (2011).

¹⁴V. M. Pereira and A. H. Castro Neto, *Phys. Rev. Lett.* **103**, 046801 (2009).

¹⁵E. Erdogan, I. Popov, C. G. Rocha, G. Cuniberti, S. Roche, and G. Seifert, *Phys. Rev. B* **83**, 041401(R) (2011).

¹⁶J. H. Warner, N. P. Young, A. I. Kirkland, and G. A. D. Briggs, *Nat. Mater.* **10**, 1 (2011).

¹⁷F. Guinea, A. K. Geim, M. I. Katsnelson, and K. S. Novoselov, *Phys. Rev. B* **81**, 035408 (2010).

¹⁸Y. C. Cheng, Z. Y. Zhu, G. S. Huang, and U. Schwingschlögl, *Phys. Rev. B* **83**, 115449 (2011).

¹⁹J. Cai, P. Ruffieux, R. Jaafar, M. Bieri, T. Braun, S. Blankenburg, M. Muoth, A. P. Seitsonen, M. Saleh, X. Feng, K. Mullen, and R. Fasel, *Nature (London)* **466**, 470 (2010).

- ²⁰D. Vanderbilt, *Phys. Rev. B* **41**, 7892 (1990).
- ²¹P. Giannozzi, S. Baroni, N. Bonini, M. Calandra, R. Car, C. Cavazzoni, D. Ceresoli, G. L. Chiarotti, M. Cococcioni, I. Dabo, A. Dal Corso, S. Fabris, G. Fratesi, S. de Gironcoli, R. Gebauer, U. Gerstmann, C. Gougoussis, A. Kokalj, M. Lazzeri, L. Martin-Samos, N. Marzari, F. Mauri, R. Mazzarello, S. Paolini, A. Pasquarello, L. Paulatto, C. Sbraccia, S. Scandolo, G. Sclauzero, A. P. Seitsonen, A. Smogunov, P. Umari, and R. M. Wentzcovitch, *J. Phys. Condens. Matter* **21**, 395502 (2009).
- ²²G. Henkelman and H. Jonsson, *J. Chem. Phys.* **113**, 9978 (2000).
- ²³J. C. Meyer, C. O. Girit, M. F. Crommie, and A. Zettl, *Nature (London)* **454**, 319 (2008).
- ²⁴J. Kotakoski, A. V. Krasheninnikov, U. Kaiser, and J. C. Meyer, *Phys. Rev. Lett.* **106**, 105505 (2011).
- ²⁵H. T. Wang, Q. X. Wang, Y. C. Cheng, K. Li, Y. B. Yao, Q. Zhang, C. Z. Dong, P. Wang, U. Schwingenschlögl, W. Yang, and X. X. Zhang, *Nano Lett.* **12**, 141 (2012).
- ²⁶H. T. Wang, K. Li, Y. C. Cheng, Q. X. Wang, Y. B. Yao, U. Schwingenschlögl, X. X. Zhang, and W. Yang (unpublished).
- ²⁷C. O. Girit, J. C. Meyer, R. Erni, M. D. Rossell, C. Kisielowski, L. Yang, C.-H. Park, M. F. Crommie, M. L. Cohen, S. G. Louie, and A. Zettl, *Science* **666**, 1705 (2009).
- ²⁸B. Song, G. F. Schneider, Q. Xu, G. Pandraud, C. Dekker, and H. Zandbergen, *Nano Lett.* **11**, 2247 (2011).
- ²⁹A. Chuvilin, U. Kaiser, E. Bichoutskaia, N. A. Besley, and A. N. Khlobystov, *Nat. Chem.* **2**, 450 (2010).
- ³⁰M. Hytch, F. Snoeck, and R. Kilaas, *Ultramicroscopy* **74**, 131 (1998).
- ³¹P. Koskinen, S. Malola, and H. Häkkinen, *Phys. Rev. Lett.* **101**, 115502 (2008).
- ³²P. Koskinen, S. Malola, and H. Häkkinen, *Phys. Rev. B* **80**, 073401 (2009).
- ³³D. Sen, K. S. Novoselov, P. M. Reis, and M. J. Buehler, *Small* **6**, 1108 (2010).
- ³⁴J. M. H. Kroes, M. A. Akhukov, J. H. Los, N. Pineau, and A. Fasolino, *Phys. Rev. B* **83**, 165411 (2011).
- ³⁵S. Baroni, S. de Gironcoli, A. Dal Corso, and P. Giannozzi, *Rev. Mod. Phys.* **73**, 515 (2001).
- ³⁶A. K. Nair, S. W. Cranford, and M. J. Buehler, *Europhys. Lett.* **95**, 16002 (2011).